



OPEN ACCESS

EDITED BY

Gokhan Zengin,
Selcuk University, Türkiye

REVIEWED BY

Prashant Murumkar,
Maharaja Sayajirao University of Baroda,
India

Syed H. Mehdi,
University of Arkansas for Medical
Sciences, United States

*CORRESPONDENCE

Jing-Jing Xu,
✉ xujingjing0224@163.com
Lin-Xi Wan,
✉ wanlx@scu.edu.cn

RECEIVED 25 August 2023

ACCEPTED 27 November 2023

PUBLISHED 08 December 2023

CITATION

Xu J-J, Luo J, Xi H, Xu J-B and Wan L-X
(2023), Palladium-catalyzed synthesis
and anti-AD biological activity evaluation
of *N*-aryl-
debenzeyldonepezil analogues.
Front. Chem. 11:1282978.
doi: 10.3389/fchem.2023.1282978

COPYRIGHT

© 2023 Xu, Luo, Xi, Xu and Wan. This is an
open-access article distributed under the
terms of the [Creative Commons
Attribution License \(CC BY\)](#). The use,
distribution or reproduction in other
forums is permitted, provided the original
author(s) and the copyright owner(s) are
credited and that the original publication
in this journal is cited, in accordance with
accepted academic practice. No use,
distribution or reproduction is permitted
which does not comply with these terms.

Palladium-catalyzed synthesis and anti-AD biological activity evaluation of *N*-aryl-debenzeyldonepezil analogues

Jing-Jing Xu^{1*}, Jiao Luo¹, Heng Xi¹, Jin-Bu Xu² and Lin-Xi Wan^{3*}

¹Department of Pharmacy, The Third People's Hospital of Chengdu, Chengdu, China, ²Sichuan Engineering Research Center for Biomimetic Synthesis of Natural Drugs, School of Life Science and Engineering, Southwest Jiaotong University, Chengdu, China, ³Sichuan Research Center for Drug Precision Industrial Technology, West China School of Pharmacy, Sichuan University, Chengdu, China

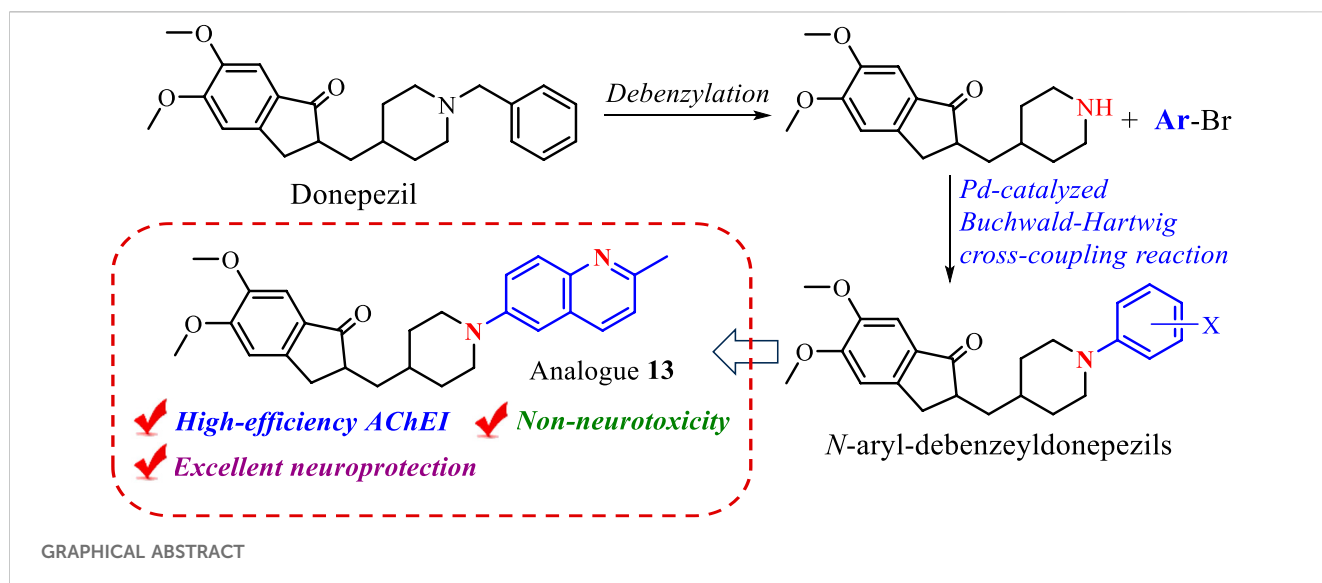
A series of novel *N*-aryl-debenzeyldonepezil derivatives (**1–26**) were designed and synthesized as cholinesterase inhibitors by the modification of anti-Alzheimer's disease drug donepezil, using Palladium catalyzed Buchwald-Hartwig cross-coupling reaction as a key chemical synthesis strategy. *In vitro* cholinesterase inhibition studies demonstrated that the majority of synthesized compounds exhibited high selective inhibition of AChE. Among them, analogue **13** possessing a quinoline functional group showed the most potent AChE inhibition effect and significant neuroprotective effect against H₂O₂-induced injury in SH-SY5Y cells. Furthermore, Compound **13** did not show significant cytotoxicity on SH-SY5Y. These results suggest that **13** is a potential multifunctional active molecule for treating Alzheimer's disease.

KEYWORDS

donepezil, Alzheimer's disease, Buchwald-Hartwig reaction, AChE, neuroprotection

1 Introduction

Alzheimer's disease (AD) is a common age-related neurodegenerative brain disorder characterized by progressive cognitive dysfunction, memory loss, and restrictions in daily activities (Ross and Poirier, 2004). According to the World Health Organization (WHO), approximately 50 million people suffer from AD disease around the world, and the number of patients will reach more than 150 million in 2050 as the population ages (Du et al., 2022). As one of the neurodegenerative disorders, the exact pathogenesis of AD is not fully known. Many studies have revealed that AD might involve abnormality of multiple neurochemical factors, such as low levels of acetylcholine (ACh), the amplitude of unusual deposits of β -amyloid ($A\beta$) peptide, hyperphosphorylated tau protein, neuronal apoptosis, and so on (Li et al., 2020; Perry et al., 2002; Lee et al., 2018; Mozaffarnia et al., 2020). Many hypotheses have been proposed based on these pathogenic factors to treat AD. The typical cholinergic hypothesis suggests that the selective loss of cholinergic neurons in the brain results in cognitive impairment in AD, whereas improvement of the central cholinergic transmission is an effective treatment strategy (Du et al., 2018). Among the several approaches attempted to enhance ACh levels in the brain, acetylcholinesterase inhibitors (AChEIs) have been proven in patients with mild or moderate AD (Anand and Singh, 2013). Up to now, donepezil, galantamine, rivastigmine, and tacrine as AChEIs have been approved by FDA used in AD



treatment (Figure 1) (Pardo-Moreno et al., 2022). Although tacrine regrettably had to be withdrawn from the market in 2005 due to its hepatotoxicity (Summers et al., 1989), all four approved AChEIs possess a basic nitrogen atom. Notably, the basic nitrogen is protonated at physiological pH to provide a temporary positive charge and interacts with the active site of AChE, generating an impact on the overall affinity of AChE for the ligands (Peauger et al., 2017). Therefore, the incorporation of a nitrogen atom in bioactive compounds to recreate their unique properties has been regarded as an effective AChEIs medicinal development route.

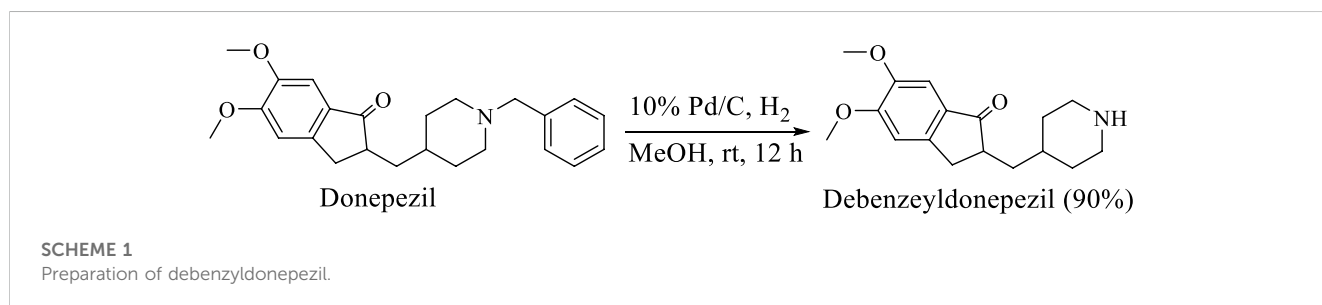
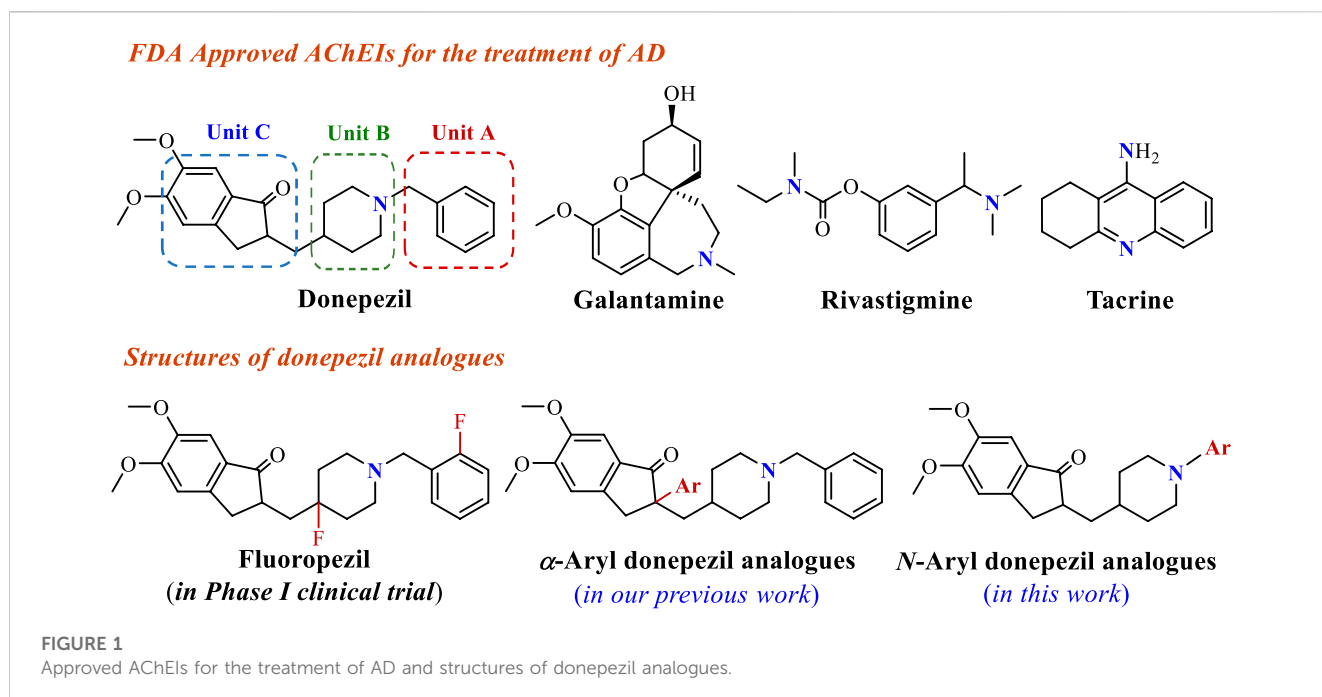
Donepezil, approved by the FDA in 1996, is a second-generation specific reversible AChEI for the treatment of mild and moderate AD, showing good patient tolerance and mild adverse effects (Seltzer, 2007). The crystal structure of donepezil-*rh*AChE complex showed benzyl moiety (Unit A) in donepezil as an important site forms π - π interactions with residues of the active site (Akhoon et al., 2020). Furthermore, the piperidine ring (Unit B) and indanone (Unit C) reach out to π - π stacking interactions with peripheral anionic and catalytic active sites of AChE (Cheung et al., 2012). These findings contribute to the cognition of potential pharmacophores interacting with the residues of the active site. With increased research enthusiasm in terms of functional AChEI molecule design, using donepezil's key structural moieties to develop novel AChEIs has drawn immense attention. For instance, fluorine-containing donepezil analogues fluoroepzil possessing a longer drug-target residence time has been developed, which is preparing to enter phase II trial (Zhou et al., 2021; Qian et al., 2023). In our previous study, various nitrogen-containing functional groups were introduced into Unit C to provide a series of α -aryl donepezil analogues owning high AChE inhibition (Wan et al., 2021a). In order to find better anti-AD compounds, considering that the aromatic ring in Unit A is a vital binding site, we envisaged using aromatic nitrogen heterocycles in place of the phenyl group might form the additional bonding force to strengthen the AChE inhibitory activity. Furthermore, the Palladium-catalyzed Buchwald-Hartwig cross-coupling reaction is one of the powerful approaches for constructing abundant structures libraries via the formation of C-N bonds and provides an important chemical ligation strategy for the present study (Dorel et al., 2019).

Therefore, as part of our ongoing research program toward exploiting novel anti-AD bioactive molecules (Wan et al., 2021a; Wan et al., 2021b; Wan et al., 2021c; Miao et al., 2021; Xu et al., 2023; Zhang et al., 2023), the present work pay attention to the AChE inhibitory activity affected by the benzyl moiety in donepezil, and proposed the structural modification of donepezil for efficiently introducing aromatic nitrogen heterocycles or aryl functional groups located at N position via Palladium-catalyzed Buchwald-Hartwig reaction, hoping to find the potential bioactive molecules. Herein, the synthesis and pharmacological evaluation of donepezil analogues are reported.

2 Results and discussion

2.1 Chemistry

To conduct the biological activity evaluation of a new class of N-aryl-debenzeyldonepezil derivatives, a set of target compound 1–26 were prepared by employing debenzeyldonepezil as a key intermediate and introducing an aryl functional group attached to the nitrogens of piperidine ring via Buchwald-Hartwig C-N cross-coupling. At the beginning of this study, donepezil was reacted with 10% Pd/C in methanol under a hydrogen atmosphere at room temperature for 4 h resulting in the generation of debenzeyldonepezil in 90% yield (Scheme 1). Next, debenzeyldonepezil and 2-bromopyridine were chosen as model substrates to explore the optimum Buchwald-Hartwig reaction conditions for the preparation of aiming N-aryl-debenzeyldonepezil. According to previous reports (Heravi et al., 2018; Dorel et al., 2019), after examination of ligands, bases, and solvents, we found that the ligand played a vital role in this C-N cross-coupling process. As shown in Table 1, the monophosphine ligands PPh₃ and PCy₃ afforded little product 1 (entries 1 and 2). The yield of the derived product was dramatically improved when using Mephos as a ligand. Therefore, the N-arylated product 1 could be received in as high as 89% yield in the presence of Pd(OAc)₂ (10 mol%), Mephos (20 mol%), and *t*-BuOK (3 equiv.) in 1,4-dioxane at 90°C for 17 h (entry 3). Then, the influence of different bases and solvents on the



reaction process was investigated. When other bases such as *t*-BuONa, K_2CO_3 , and KF were used instead of *t*-BuOK, the desired cross-coupling product **1** was obtained in unsatisfactory yields (entries 4–6). Similarly, replacing 1,4-dioxane with DME and THF provided a lower yield of 37% and 23%, respectively (entries 7 and 8).

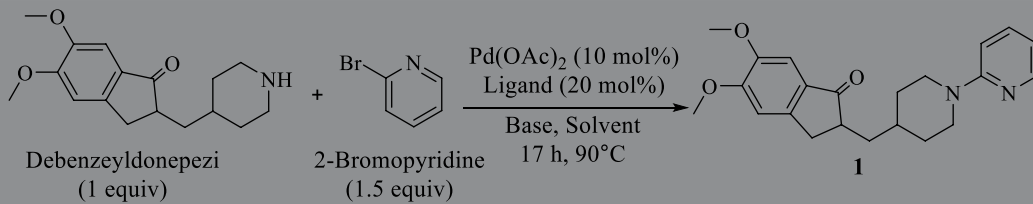
Subsequently, Palladium-catalyzed Buchwald-Hartwig reactions between debenzyldonepezil and various aryl bromides were conducted under standard reaction conditions. As exemplified in **Scheme 2**, the investigated *N*-heteroaryl bromides smoothly provided the corresponding *N*-arylated debenzyldonepezil products **1–13** in excellent yields (65%–89%). Both electron-donating groups (methyl and methoxy) and halogen fluorine at *meta*-, *para*- or *ortho*-position of 2-bromopyridine were well tolerated. The bromide substrates bearing a multisubstituted ring were tested and afforded the expected products **3** and **5** in 77% and 69% yields, respectively. Meanwhile, quinoline groups were suitable as well in this process to furnish corresponding products in yields of 72% (**11**), 75% (**12**), and 68% (**13**). In addition to pyridine and quinoline bromides, the substrates carrying phenyl rings were examined and provided the conjugate products in 50–92% yield (**14–26**). The unsubstituted benzene-bromide furnished the derivative **14** in 89% yield. Similarly, the phenyl bromides

bearing electron-donating groups (methyl, methoxy, and tertiary butyl) (**15–18**) worked efficiently. The substrates carrying electron-withdrawing groups (fluorine and trifluoromethyl) (**19–23**) were in lower yields in comparison to that of **15–18**. Compounds **24** and **25** equipped biphenyl groups were successfully prepared in yields of 79% and 69%, respectively. Furthermore, the reaction of debenzyldonepezil with 1-bromo-4-methoxynaphthalene gave compound **26** an 80% yield. Structures of these *N*-aryl-debenzyldonepezil analogues were characterized by NMR and HRESIMS spectra.

2.2 Biological activities

2.2.1 *In vitro* cholinesterase inhibition studies

The inhibitory activity of *N*-aryl-debenzyldonepezil analogues (**1–26**) against AChE (from electric eel) was initially evaluated by means of Ellman's spectrophotometric method (Ellman et al., 1961), employing donepezil as the positive control. The screening test was conducted at the concentrations of 100 and 50 μ M, and the ability of these molecules to inhibit the enzymes is reported in **Table 2**. When introducing methylpyridine-provided compounds **2–5**, the AChE

TABLE 1 Optimization of the *N*-arylation reaction conditions^a.


Entry	Ligand	Base	Solvent	Yield (%) ^b
1	PPh ₃	<i>t</i> -BuOK	Dioxane	<5
2	PCy ₃	<i>t</i> -BuOK	Dioxane	<5
3	Mephos	<i>t</i>-BuOK	Dioxane	89
4	Mephos	<i>t</i> -BuONa	Dioxane	10
5	Mephos	K ₂ CO ₃	Dioxane	<5
6	Mephos	KF	Dioxane	<5
7	Mephos	<i>t</i> -BuOK	DME	37
8	Mephos	<i>t</i> -BuOK	THF	23

^aReaction conditions: debenzeyldonepezi (0.1 mmol, 1.0 equiv.), 3-bromopyridine (0.15 mmol, 1.5 equiv.), Pd(OAc)₂ (10 mol%), ligand (20 mol%), and base (0.3 mmol, 3 equiv.) in 2 mL solvent at 90°C for 17 h under argon atmosphere.

^bIsolated yield.

Bold values indicates the best reaction condition.

inhibition activity of them was obviously lower than that of pyridine-substituted analogue **1**. For the position of the methoxyl substituent group, compounds **8** with 4-methoxy pyridine and **9** with 3-methoxypyridine obtained maintenance in activity, while the activity of **6** (6-methoxypyridine) and **7** (5-methoxypyridine) decreased. The only compound **10** (*EeAChE* inhibitory rate = 44.1 ± 3.0% at 50 μM) in the series bearing a strong electron-withdrawing group also resulted in a larger decrease of AChE inhibitory activity than analogue **1**. The above results implied that the steric effects of these substituent groups possibly combining with electronic effects led to an adverse impact on the inhibition potency for this set of analogues. In short, the *N*-aryl-debenzeyldonepezils **1–10** equipping pyridine ring showed slightly decreased AChE inhibitory capacity, compared to that of donepezil, which revealed that the introduction of pyridine is at a significant disadvantage.

On the other hand, for the analogues possessing the quinoline fragments, compounds **11–13** exhibited favorable inhibitory activities, implying that the presence of this basic atomic group could increase interactions with the active sites of the enzymes. Compound **13** showed the best inhibitory potency, which needs an in-depth investigation. Many studies of AChE crystal structures have confirmed that the active site gorge is located in the deep and narrow “canyon” (Cheung et al., 2012; Liu et al., 2022), which implied that the larger group 2-methylquinoline might contribute to occupying the active site and obtaining compound **13** with high activity against AChE. Moreover, most compounds of the phenyl series (**14–23**) showed moderate inhibition effect against AChE. Introducing electron-withdrawing groups into the benzene ring, as shown in compounds **19–23**, improved activity more than that of analogues with electron-donating groups (**15–18**), probably due to electronic effects. However, two diphenyl analogues (**24** and **25**) among this subset of

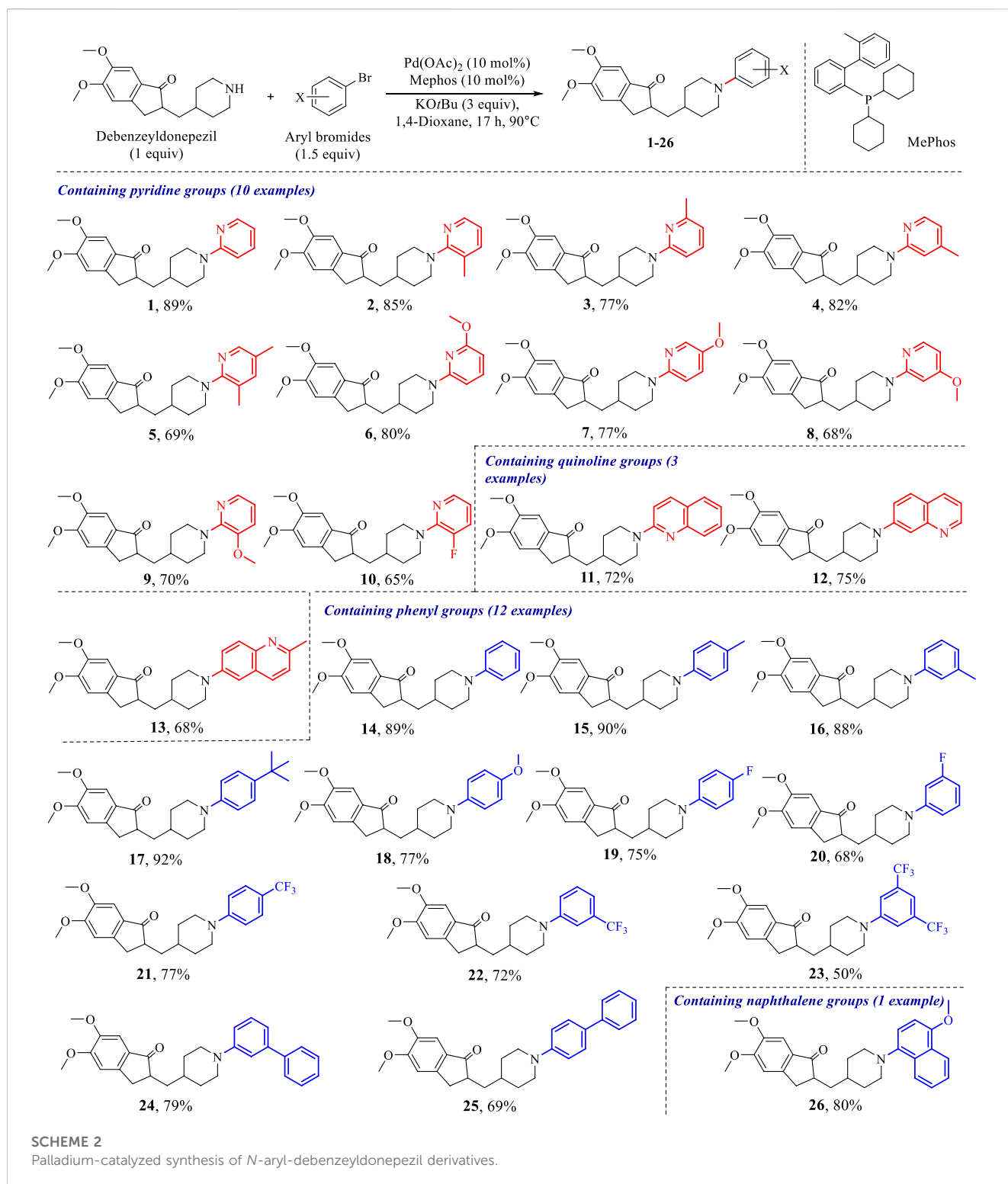
compounds seem to be noneffective, showing an *EeAChE* inhibitory rate of only about 50% at 50 μM. Then, the *EqBuChE* inhibition effects of these *N*-aryl-debenzeyldonepezil derivatives were also explored. As expected, all of them showed low inhibitory activity against *eqBuChE*.

2.2.2 Molecular modelling studies

To explore the binding mechanisms of compound **13** on AChE (PDB ID code: 1acj), a docking study to reveal the sites of binding and relative binding energy was performed. The highest-scored pose of **13** with a binding energy of −6.9 kcal/mol is depicted in Figure 2. Molecular docking results indicated that analogue **13** was suitably filled in the active site of AChE. Two π-alkyl hydrophobic interactions were formed by the quinoline fragment with Tyr 70 and Tyr 121, respectively. The benzene ring from quinoline established a π-anion bond with Asp 72. Moreover, attempt 334 was in a favorable position of stacking with the piperidine ring and quinoline's benzene ring, forming a π-π and a π-alkyl interactions. Comparatively, in the active cavity of BuChE (PDB ID code: 6ASM), only the benzene ring from indanone interacted with Val 348 by π-alkyl interaction, and the carbonyl showed a conventional hydrogen bond with residues Arg 132. The highest-scored pose of **13** presented a binding energy of −5.6 kcal/mol (Figure 3). The above results could explain the compound **13** possessed the selective AChE inhibitory activity, which verified the *in vitro* enzyme inhibitory assay.

2.2.3 Neuroprotection effects against H₂O₂-induced injury in SH-SY5Y cells

The death of neuronal cells is the central abnormality occurring in brains suffering from AD (Niikura et al., 2002). Neuroprotection is a useful way to protect the neuronal cells from damage, which potentially slows down or prevents the



progression of AD (Coleman et al., 2004). To explore the therapeutic potential of synthesized analogues 1–26, the neuroprotective effects of 1–26 against H₂O₂-induced injury in SH-SY5Y cells were performed. Firstly, the neurotoxicity of compounds 1–26 on SH-SY5Y cell viability was determined using the MTT assay method. As shown in Table 3, *N*-aryl-debenzylonepezils 6–8, 17–22, and 26 did not affect the cell

viability of SH-SY5Y cells even at concentrations up to 50 μM, indicating that they were not neurotoxic. Then, non-cytotoxic compounds (6–8, 17–22, and 26) were examined for their potential neuroprotective activity on damaged SH-SY5Y cellular models induced by 700 μM H₂O₂. In the model group, 700 μM H₂O₂ significantly reduced cell viability and decreased to 61% compared to the control group. The protective effect of analogues

TABLE 2 Cholinesterase Inhibitory Activities of *N*-aryl-debenzylonepezil analogues.

Compound	<i>Ee</i> AChE inhibitory rate (IR) [%] ^a		<i>Eq</i> BuChE inhibitory rate (IR) [%] ^a	
	[I] = 100 μ M	[I] = 50 μ M	[I] = 100 μ M	[I] = 50 μ M
1	86.3 \pm 3.0	58.3 \pm 2.8	40.0 \pm 2.1	19.4 \pm 2.7
2	82.7 \pm 2.8	52.1 \pm 0.9	31.0 \pm 3.3	-19.6 \pm 1.3
3	82.2 \pm 3.2	52.9 \pm 3.2	37.9 \pm 2.7	31.3 \pm 1.0
4	84.4 \pm 1.5	39.0 \pm 2.7	33.5 \pm 2.7	36.1 \pm 2.4
5	84.2 \pm 2.6	49.2 \pm 3.2	29.0 \pm 2.2	26.5 \pm 3.7
6	87.4 \pm 4.0	42.9 \pm 2.0	0.9 \pm 1.5	27.9 \pm 1.3
7	86.4 \pm 1.4	49.3 \pm 1.9	13.1 \pm 0.6	25.9 \pm 2.4
8	83.1 \pm 2.8	59.4 \pm 1.0	11.7 \pm 1.7	29.4 \pm 3.7
9	82.3 \pm 3.0	59.8 \pm 1.1	9.4 \pm 2.0	37.2 \pm 0.9
10	77.7 \pm 1.9	44.1 \pm 3.0	6.8 \pm 3.9	24.1 \pm 2.3
11	87.3 \pm 1.7	61.1 \pm 2.1	24.6 \pm 2.0	13.7 \pm 2.8
12	84.5 \pm 1.2	59.0 \pm 1.7	16.9 \pm 3.7	30.4 \pm 1.7
13	89.0 \pm 2.2	74.4 \pm 3.5	40.3 \pm 2.3	12.7 \pm 2.0
14	81.1 \pm 2.8	42.8 \pm 3.7	13.3 \pm 1.0	23.8 \pm 2.2
15	78.5 \pm 1.1	47.8 \pm 2.8	-26.7 \pm 1.8	35.8 \pm 2.7
16	74.9 \pm 2.0	52.9 \pm 1.9	17.9 \pm 2.1	2.1 \pm 3.2
17	75.0 \pm 3.1	53.7 \pm 1.2	14.4 \pm 3.2	4.5 \pm 2.0
18	65.5 \pm 2.1	53.0 \pm 1.1	25.3 \pm 2.2	5.1 \pm 2.3
19	64.1 \pm 3.2	61.9 \pm 3.5	20.9 \pm 2.9	11.9 \pm 2.5
20	71.6 \pm 3.9	57.1 \pm 2.9	68.8 \pm 1.0	1.1 \pm 1.9
21	65.6 \pm 1.0	56.9 \pm 1.5	1.7 \pm 3.6	1.3 \pm 2.7
22	53.0 \pm 0.9	59.3 \pm 0.9	14.6 \pm 2.9	-5.4 \pm 3.2
23	60.3 \pm 1.5	62.4 \pm 2.0	3.5 \pm 1.6	-18.8 \pm 3.9
24	81.5 \pm 2.9	50.4 \pm 3.9	14.1 \pm 1.9	1.2 \pm 1.9
25	78.6 \pm 1.0	50.7 \pm 0.8	-3.8 \pm 2.7	0.4 \pm 2.5
26	68.1 \pm 3.0	58.0 \pm 2.3	18.8 \pm 1.5	-4.9 \pm 1.0
Donepezil	87.2 \pm 1.2	66.9 \pm 2.9	27.8 \pm 2.8	25.3 \pm 1.3

^aPercent inhibition data are the mean \pm SD, of three independent experiments each performed in duplicate.

6–8, 17–22, and 26 against H₂O₂ are shown in Table 4. The survival rate of damaged SH-SY5Y cells increased to 115% after the following treatment of compound 13, suggesting that synthetic compound 13 can protect cells against H₂O₂-induced cell death.

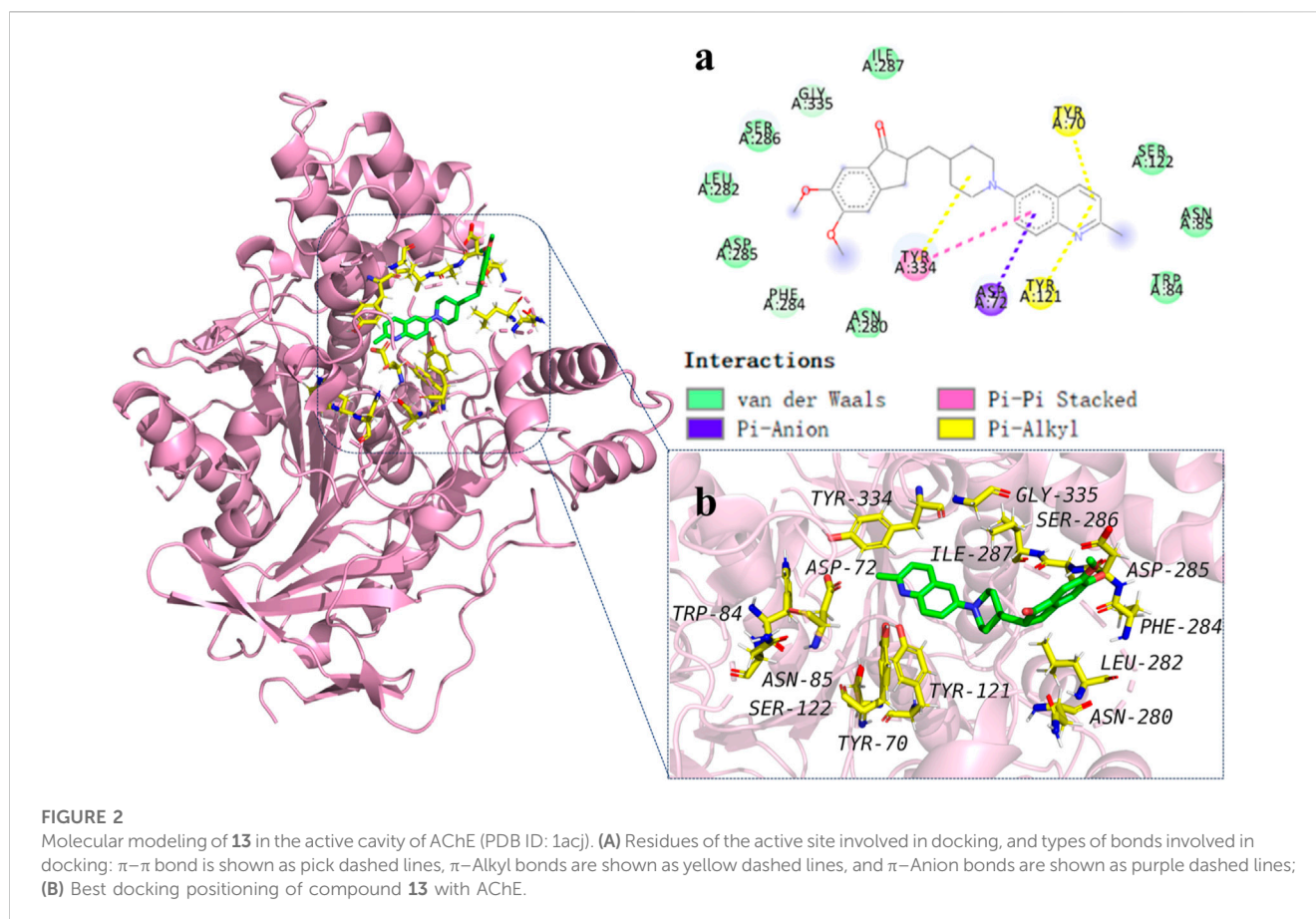
2.2.4 BBB prediction

Penetrating the blood-brain barrier (BBB) is extremely significant for anti-AD medicines, so the BBB penetration of compounds 1–26 was predicted by using Calculate Molecular Properties (Discovery Studio 2020 Client). The predicted data are listed in Table 5. The level “0” shows that the Brain-Blood ratio is greater than 5:1, the value “1” expresses that the Brain-Blood ratio is between 1:1 and 5:1, and the value “2” expresses that the Brain-

Blood ratio is between 0.3:1 and 1:1. Besides compound 11, most of the synthesized compounds are BBB permeable.

3 Conclusion

In summary, a series of new *N*-aryl-debenzylonepezil analogues (1–26) were efficiently synthesized in modification of donepezil by using Palladium-catalyzed Suzuki-Miyaura cross-coupling reaction as a key synthetic method. The cholinesterase inhibition and neuroprotective effects of these analogues were evaluated to develop potential candidate molecules for the treatment of AD. Among them, compound 13 exhibited good



selective inhibitory activities against AChE, which might be attributed to the introduction of nitrogen-containing aromatic heterocycle. Molecular modeling was performed to explain the possible interaction between compound **13** and AChE. The prediction of bioavailability disclosed that analogue **13** had a favorable capacity to pass through the blood-brain barrier (BBB). Furthermore, further study showed that active compound **13** displayed non-neurotoxicity and good neuroprotective potency against H_2O_2 -induced injury in SH-SY5Y cells. These results showed that compound **13** could be developed as an efficient multifunctional potential active molecule for the treatment of AD.

4 Experimental section

4.1 Chemistry

4.1.1 Materials and methods

All reactions were conducted under an inert atmosphere of dry argon. Anhydrous THF was purchased from Aladdin and used without further purification. Unless otherwise noted, the reagents and solvents used in this article were all commercially available analytical or chemical grades and used directly without any purification. Reactions were monitored by thin layer chromatography (TLC) on silica gel plates (GF 254) using UV light to visualize the course of the reactions. Silica gel H (Qingdao Sea Chemical Factory, Qingdao, PR China) was used

for column chromatography. NMR spectra were recorded by using a Bruker AV 400 or 600 nuclear magnetic resonance instrument. Chemical shifts (δ) were recorded in ppm relative to TMS as the internal standard. HRESIMS spectra were recorded on a Waters Acquity UPLC/Q-TOF micro mass spectrometer.

4.1.2 Synthesis of debenzeyldonepezil

Donepezil (2.635 mmol) was suspended in 40 mL of a MeOH solution. To the reaction was added 10% Pd/C (0.2635 mmol), stirred at 25°C under an argon atmosphere for 12 h. Then, the mixture was filtered and evaporated under a vacuum. The reaction crude product was purified by flash column chromatography using PE-EA (3:1 to 1:1) to obtain debenzeyldonepezil as amorphous powder (90% yield); ^1H NMR (400 MHz, CDCl_3) δ 7.16 (s, 1H), 6.85 (s, 1H), 3.95 (s, 3H), 3.89 (s, 3H), 3.23 (dd, $J = 17.4, 8.0$ Hz, 1H), 3.09 (t, $J = 9.6$ Hz, 2H), 2.74–2.67 (m, 2H), 2.63–2.57 (m, 2H), 1.92–1.86 (m, 1H), 1.77 (d, $J = 13.2$ Hz, 1H), 1.69 (d, $J = 13.2$ Hz, 1H), 1.69 (d, $J = 13.2$ Hz, 1H), 1.34–1.24 (m, 2H), 1.22–1.11 (m, 2H); ^{13}C NMR (100 MHz, CDCl_3) δ 208.0, 155.6, 149.6, 148.9, 129.4, 107.5, 104.5, 56.3, 56.2, 46.9, 46.8, 45.3, 39.5, 35.0, 34.4, 33.4, 33.1; HRESIMS m/z 290.1740 [$\text{M} + \text{H}$] $^+$ (calcd for $\text{C}_{17}\text{H}_{24}\text{NO}_3$, 290.1756).

4.1.3 Synthesis of *N*-aryl-debenzeyldonepezil analogues 1–26

The suspension of $\text{Pd}(\text{OAc})_2$ (5 mol%) and Mephos (10 mol%) in anhydrous 1,4-dioxane (3 mL) was stirred at 30°C under an argon atmosphere for 2 h to obtain a brown solution. The brown solution

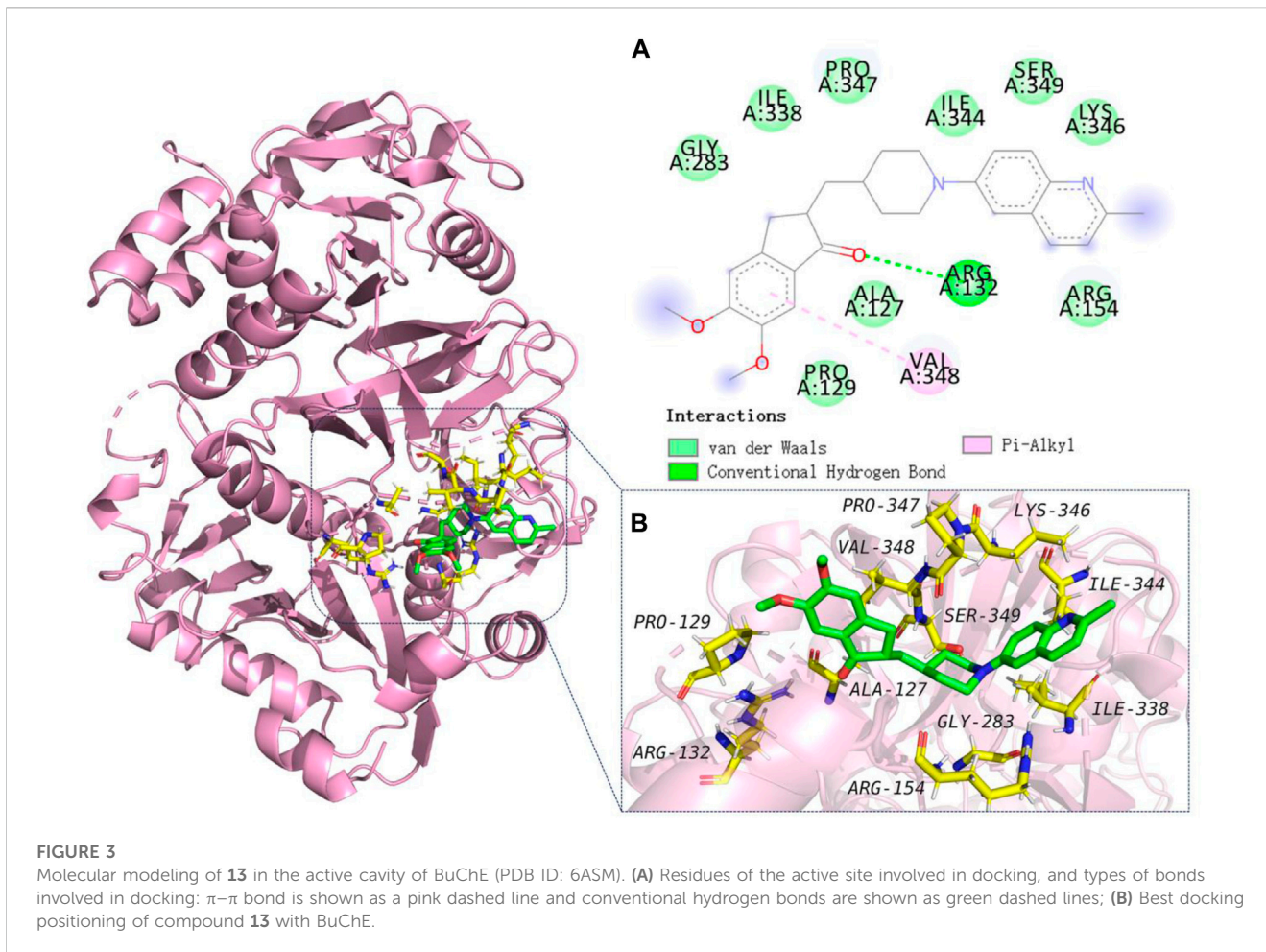


TABLE 3 Toxicity of compounds 1–26 on SH-SY5Y cells at 50 μ M.

Compound	Cell viability (%) ^a	Compound	Cell viability (%) ^a
1	47.1 ± 1.1	14	112.0 ± 2.3
2	83.3 ± 1.1	15	101.8 ± 2.9
3	77.6 ± 4.7	16	81.1 ± 3.2
4	74.4 ± 1.4	17	103.1 ± 1.9
5	66.1 ± 0.5	18	109.6 ± 3.1
6	98.6 ± 1.5	19	99.6 ± 1.7
7	103.8 ± 2.9	20	100.2 ± 0.9
8	109.2 ± 2.2	21	96.5 ± 1.2
9	76.8 ± 2.5	22	91.5 ± 0.3
10	101.0 ± 2.6	23	56.8 ± 4.0
11	91.2 ± 4.9	24	85.1 ± 1.9
12	77.2 ± 3.0	25	66.6 ± 1.3
13	112.1 ± 1.9	26	103.3 ± 2.2

^aData are the means ± SD, of at least three determinations.

TABLE 4 Neuroprotective effect of non-cytotoxic compounds against H₂O₂-induced injury in SH-SY5Y cells^a.

Compound	Cell viability (%) ^b	Compound	Cell viability (%) ^b
6	44.6 ± 2.0	17	68.4 ± 2.3
7	45.5 ± 1.2	18	56.0 ± 1.5
8	43.3 ± 4.0	19	44.3 ± 3.9
10	41.3 ± 2.5	20	37.0 ± 2.2
11	56.0 ± 3.5	21	42.5 ± 1.9
13	115.3 ± 2.7	22	45.9 ± 2.6
14	52.6 ± 3.0	26	41.3 ± 1.7
15	49.3 ± 2.0		

^aNeuroprotective effect of compounds (50 μM) on H₂O₂-induced (700 μM) neurotoxicity in SH-SY5Y cells. The cell viability in the control was taken as 100%, and the average value of cell viability under H₂O₂ exposure in the model group was 61.2% ± 1.3% (*n* = 3).

^bData are the means ± SD, of at least three determinations.

TABLE 5 The BBB prediction of compounds by Discovery Studio 2020 Client.

Compound	Level	ADMET_BBB	Compound	Level	ADMET_BBB
1	1	0.142	14	1	0.163
2	1	0.459	15	1	0.163
3	1	0.459	16	1	0.373
4	1	0.396	17	1	0.676
5	0	1.259	18	0	1.109
6	0	0.722	19	0	1.146
7	1	0.556	20	1	0.530
8	1	0.643	21	0	0.811
9	1	0.329	22	0	0.740
10	1	0.163	23	0	0.740
11	2	-0.156	24	0	0.827
12	1	0.649	25	0	0.827
13	1	0.610	26	0	1.146
Donepezil	0	0.649			

was added to a 10 mL sealed dry reaction vial containing debenzyldonepezil (1 mmol), naphthalenyl bromides (1.5 mmol), and *t*-BuOK (3 mmol) via a syringe. The reaction mixture was stirred for 17 h at 90°C before quenching with two drops of H₂O. Then, the mixture was diluted with ethyl acetate (3 mL), and filtered over a pad of MgSO₄. The pad was rinsed with ethyl acetate, and the mixture was concentrated *in vacuo*. The reaction crude product was purified by flash column chromatography using PE-EA (2:1-1:2) to obtain the *N*-aryl-debenzyldonepezil analogues 1–26 (50%–89% yields).

Compound 1, amorphous powder, 89% yield; ¹H NMR (400 MHz, CDCl₃) δ 8.18–8.16 (m, 1H), 7.44–7.42 (m, 1H), 7.17 (s, 1H), 6.86 (s, 1H), 6.66 (d, *J* = 8.4 Hz, 1H), 6.57–6.55 (m, 1H), 4.33–4.28 (m, 2H), 3.96 (s, 3H), 3.90 (s, 3H), 3.31 (q, *J* = 8.4 Hz, 1H), 2.87–2.79 (m, 2H), 2.77–2.70 (m, 2H), 1.97–1.90 (m, 1H), 1.87–1.78 (m, 2H), 1.40–1.25 (m, 4H); ¹³C NMR (100 MHz, CDCl₃)

δ 207.8, 159.8, 155.7, 149.7, 148.9, 148.2, 137.6, 129.5, 112.9, 107.6, 107.4, 104.6, 56.4, 56.3, 45.9, 45.9, 45.5, 39.0, 35.0, 33.6, 32.8, 31.6; HRESIMS *m/z* 367.2012 [M + H]⁺ (calcd for C₂₂H₂₇N₂O₃, 367.2022).

Compound 2, amorphous powder, 85% yield; ¹H NMR (400 MHz, CDCl₃) δ 8.15–8.14 (m, 1H), 7.39–7.37 (m, 1H), 7.18 (s, 1H), 6.87 (s, 1H), 6.82 (dd, *J* = 7.2, 4.8 Hz, 1H), 3.96 (s, 3H), 3.91 (s, 3H), 3.49–3.42 (m, 2H), 3.28 (q, *J* = 8.4 Hz, 1H), 2.83–2.73 (m, 4H), 2.26 (s, 3H), 2.02–1.96 (m, 1H), 1.91–1.77 (m, 2H), 1.53–1.36 (m, 4H); ¹³C NMR (100 MHz, CDCl₃) δ 207.9, 162.6, 155.7, 149.6, 148.9, 145.3, 139.2, 129.5, 125.3, 117.7, 107.5, 104.6, 56.4, 56.2, 50.39, 50.38, 45.6, 39.0, 34.8, 33.7, 33.4, 32.3, 18.4; HRESIMS *m/z* 381.2162 [M + H]⁺ (calcd for C₂₃H₂₉N₂O₃, 381.2178).

Compound 3, amorphous powder, 77% yield; ¹H NMR (400 MHz, CDCl₃) δ 7.34 (t, *J* = 8.4 Hz, 1H), 7.18 (s, 1H), 6.87 (s, 1H), 6.45 (d, *J* = 2.7 Hz, 1H), 6.43 (s, 1H), 4.35–4.30 (m, 2H), 3.96

(s, 3H), 3.91 (s, 3H), 3.29 (q, $J = 8.0$ Hz, 1H), 2.83–2.79 (m, 1H), 2.78–2.71 (m, 3H), 2.39 (s, 3H), 1.97–1.90 (m, 1H), 1.86–1.77 (m, 2H), 1.40–1.30 (m, 4H); ^{13}C NMR (100 MHz, CDCl_3) δ 207.8, 159.5, 156.9, 155.7, 149.6, 148.9, 137.8, 129.4, 112.2, 107.5, 104.6, 104.0, 56.3, 56.2, 46.0, 45.9, 45.4, 38.9, 35.0, 33.5, 32.8, 31.6, 24.7; HRESIMS m/z 381.2165 $[\text{M} + \text{H}]^+$ (calcd for $\text{C}_{23}\text{H}_{29}\text{N}_2\text{O}_3$, 381.2178).

Compound **4**, amorphous powder, 82% yield; ^1H NMR (400 MHz, CDCl_3) δ 8.04 (d, $J = 5.2$ Hz, 1H), 7.18 (s, 1H), 6.87 (s, 1H), 6.48 (s, 1H), 6.43 (d, $J = 5.2$ Hz, 1H), 4.31–4.27 (m, 2H), 3.96 (s, 3H), 3.91 (s, 3H), 3.31 (q, $J = 9.2$ Hz, 1H), 2.85–2.79 (m, 2H), 2.78–2.70 (m, 2H), 2.25 (s, 3H), 1.97–1.90 (m, 1H), 1.87–1.77 (m, 2H), 1.40–1.29 (m, 4H); ^{13}C NMR (100 MHz, CDCl_3) δ 207.8, 160.0, 155.7, 149.6, 148.9, 148.4, 147.7, 129.4, 114.4, 107.8, 107.5, 104.6, 56.4, 56.3, 46.1, 46.0, 45.4, 39.0, 35.0, 33.5, 32.7, 31.6, 21.6; HRESIMS m/z 381.2163 $[\text{M} + \text{H}]^+$ (calcd for $\text{C}_{23}\text{H}_{29}\text{N}_2\text{O}_3$, 381.2178).

Compound **5**, amorphous powder, 69% yield; ^1H NMR (400 MHz, CDCl_3) δ 7.96 (d, $J = 2.0$ Hz, 1H), 7.22 (d, $J = 2.0$ Hz, 1H), 7.19 (s, 1H), 6.88 (s, 1H), 3.97 (s, 3H), 3.91 (s, 3H), 3.40–3.35 (m, 2H), 3.29 (q, $J = 8.0$ Hz, 1H), 2.79–2.73 (m, 4H), 2.24 (s, 3H), 2.21 (s, 3H), 2.02–1.96 (m, 1H), 1.90–1.76 (m, 2H), 1.53–1.37 (m, 4H); ^{13}C NMR (100 MHz, CDCl_3) δ 208.0, 160.7, 155.6, 149.6, 149.0, 145.2, 140.2, 129.5, 127.0, 125.0, 107.5, 104.6, 56.4, 56.3, 50.8, 50.7, 45.7, 39.0, 34.8, 33.7, 33.4, 32.3, 18.1, 17.6; HRESIMS m/z 395.2321 $[\text{M} + \text{H}]^+$ (calcd for $\text{C}_{24}\text{H}_{31}\text{N}_2\text{O}_3$, 395.2335).

Compound **6**, amorphous powder, 80% yield; ^1H NMR (400 MHz, CDCl_3) δ 7.37 (t, $J = 8.0$ Hz, 1H), 7.17 (s, 1H), 6.86 (s, 1H), 6.16 (d, $J = 8.0$ Hz, 1H), 6.02 (d, $J = 8.0$ Hz, 1H), 4.33–4.27 (m, 2H), 3.96 (s, 3H), 3.90 (s, 3H), 3.85 (s, 3H), 3.28 (q, $J = 9.2$ Hz, 1H), 2.83–2.71 (m, 4H), 1.96–1.89 (m, 1H), 1.85–1.76 (m, 2H), 1.40–1.24 (m, 4H); ^{13}C NMR (100 MHz, CDCl_3) δ 207.7, 163.2, 158.5, 155.6, 149.6, 148.8, 140.1, 129.4, 107.5, 104.5, 98.3, 97.4, 56.3, 56.2, 53.0, 45.8, 45.7, 45.4, 38.9, 34.9, 33.5, 32.6, 31.5; HRESIMS m/z 397.2116 $[\text{M} + \text{H}]^+$ (calcd for $\text{C}_{23}\text{H}_{29}\text{N}_2\text{O}_4$, 397.2127).

Compound **7**, amorphous powder, 77% yield; ^1H NMR (400 MHz, CDCl_3) δ 7.93 (d, $J = 3.2$ Hz, 1H), 7.18 (s, 1H), 7.13 (dd, $J = 6.0, 2.8$ Hz, 1H), 6.87 (s, 1H), 6.66 (d, $J = 8.8$ Hz, 1H), 4.16–4.10 (m, 2H), 3.96 (s, 3H), 3.91 (s, 3H), 3.79 (s, 3H), 3.31 (q, $J = 9.2$ Hz, 1H), 2.81–2.77 (m, 2H), 2.76–2.71 (m, 2H), 1.97–1.91 (m, 1H), 1.88–1.78 (m, 2H), 1.44–1.30 (m, 4H); ^{13}C NMR (100 MHz, CDCl_3) δ 207.9, 155.7, 155.6, 149.7, 149.0, 148.9, 133.8, 129.5, 125.2, 108.7, 107.6, 104.6, 56.5, 56.4, 56.3, 47.2, 47.1, 45.5, 39.0, 34.9, 33.6, 32.8, 31.6; HRESIMS m/z 397.2110 $[\text{M} + \text{H}]^+$ (calcd for $\text{C}_{23}\text{H}_{29}\text{N}_2\text{O}_4$, 397.2127).

Compound **8**, amorphous powder, 68% yield; ^1H NMR (400 MHz, CDCl_3) δ 8.03 (d, $J = 5.8$ Hz, 1H), 7.17 (s, 1H), 6.86 (s, 1H), 6.21 (dd, $J = 5.8, 2.2$ Hz, 1H), 6.12 (d, $J = 2.2$ Hz, 1H), 4.30–4.24 (m, 2H), 3.96 (s, 3H), 3.90 (s, 3H), 3.80 (s, 3H), 3.31 (q, $J = 9.2$ Hz, 1H), 2.86–2.78 (m, 2H), 2.75–2.71 (m, 2H), 1.96–1.90 (m, 1H), 1.86–1.77 (m, 2H), 1.40–1.29 (m, 4H); ^{13}C NMR (100 MHz, CDCl_3) δ 207.8, 167.4, 161.6, 155.7, 149.6, 149.2, 148.8, 129.4, 107.5, 104.6, 100.7, 92.1, 56.4, 56.2, 55.0, 46.1, 46.0, 45.4, 38.9, 35.0, 33.5, 32.7, 31.5; HRESIMS m/z 397.2117 $[\text{M} + \text{H}]^+$ (calcd for $\text{C}_{23}\text{H}_{29}\text{N}_2\text{O}_4$, 397.2127).

Compound **9**, amorphous powder, 70% yield; ^1H NMR (400 MHz, CDCl_3) δ 7.86 (dd, $J = 3.6, 1.2$ Hz, 1H), 7.18 (s, 1H), 7.01 (dd, $J = 6.4, 1.6$ Hz, 1H), 6.87 (s, 1H), 6.81 (dd, $J = 8.0, 4.8$ Hz, 1H), 3.96 (s, 3H), 3.94–3.92 (m, 2H), 3.90 (s, 3H), 3.84 (s, 3H), 3.28 (q, $J = 9.2$ Hz, 1H), 2.80–2.72 (m, 4H), 2.01–1.94 (m, 1H), 1.88–1.76

(m, 2H), 1.57–1.34 (m, 4H); ^{13}C NMR (100 MHz, CDCl_3) δ 207.9, 155.6, 153.0, 149.6, 148.9, 147.2, 138.9, 129.5, 117.5, 116.8, 107.5, 104.6, 56.3, 56.2, 55.4, 49.1, 49.0, 45.6, 39.0, 35.0, 33.5, 33.3, 32.0; HRESIMS m/z 397.2114 $[\text{M} + \text{H}]^+$ (calcd for $\text{C}_{23}\text{H}_{29}\text{N}_2\text{O}_4$, 397.2127).

Compound **10**, amorphous powder, 65% yield; ^1H NMR (400 MHz, CDCl_3) δ 7.97–7.94 (m, 1H), 7.24–7.10 (m, 2H), 6.85 (d, $J = 2.0$ Hz, 1H), 6.73–6.66 (m, 1H), 4.14–4.02 (m, 2H), 3.94 (s, 3H), 3.89 (s, 3H), 3.32–3.17 (m, 1H), 2.94–2.66 (m, 4H), 1.98–1.92 (m, 1H), 1.87–1.73 (m, 2H), 1.49–1.37 (m, 4H); ^{13}C NMR (100 MHz, CDCl_3) δ 208.0, 158.2, 149.6 (d, $J = 30$ Hz), 142.8 (d, $J = 5$ Hz), 142.6 (d, $J = 60$ Hz), 131.4, 129.4, 123.1 (d, $J = 19$ Hz), 115.8, 107.5, 104.5, 56.3, 56.2, 48.8, 48.7, 45.5, 39.1, 34.9, 33.5, 33.3, 31.9, 28.8; HRESIMS m/z 385.1911 $[\text{M} + \text{H}]^+$ (calcd for $\text{C}_{22}\text{H}_{26}\text{FN}_2\text{O}_3$, 385.1927).

Compound **11**, amorphous powder, 72% yield; ^1H NMR (400 MHz, CDCl_3) δ 7.86 (d, $J = 10.0$ Hz, 1H), 7.69 (d, $J = 8.4$ Hz, 1H), 7.58 (dd, $J = 6.4, 1.2$ Hz, 1H), 7.51–7.49 (m, 1H), 7.20–7.20 (m, 1H), 7.18 (s, 1H), 7.01 (d, $J = 9.2$ Hz, 1H), 6.87 (s, 1H), 4.59–4.56 (m, 2H), 3.97 (s, 3H), 3.91 (s, 3H), 3.32–3.24 (q, $J = 8.4$ Hz, 1H), 3.00–2.93 (m, 2H), 2.79–2.72 (m, 2H), 1.99–1.92 (m, 1H), 1.90–1.83 (m, 2H), 1.42–1.31 (m, 4H); ^{13}C NMR (100 MHz, CDCl_3) δ 207.7, 157.7, 155.7, 149.7, 148.8, 137.4, 129.5, 129.4, 127.3, 127.2, 126.7, 123.0, 122.2, 110.0, 107.5, 104.6, 56.4, 56.3, 45.8, 45.4, 45.3, 38.9, 35.1, 33.6, 32.9, 31.8; HRESIMS m/z 417.2166 $[\text{M} + \text{H}]^+$ (calcd for $\text{C}_{26}\text{H}_{29}\text{N}_2\text{O}_3$, 417.2178).

Compound **12**, amorphous powder, 75% yield; ^1H NMR (400 MHz, CDCl_3) δ 8.88 (dd, $J = 4.2, 1.8$ Hz, 1H), 8.50 (d, $J = 7.6$ Hz, 1H), 7.79 (d, $J = 8.4$ Hz, 1H), 7.61 (t, $J = 7.6$ Hz, 1H), 7.38 (dd, $J = 8.6, 4.0$ Hz, 1H), 7.20 (s, 1H), 7.12 (d, $J = 6.4$ Hz, 1H), 6.88 (s, 1H), 3.97 (s, 3H), 3.92 (s, 3H), 3.41–3.35 (m, 2H), 3.34–3.27 (m, 1H), 2.83–2.75 (m, 4H), 2.08–2.03 (m, 1H), 1.97–1.87 (m, 2H), 1.71–1.62 (m, 4H); ^{13}C NMR (100 MHz, CDCl_3) δ 207.8, 155.7, 150.9, 150.2, 149.7, 149.6, 148.9, 132.6, 129.5, 129.4, 124.4, 120.3, 115.2, 115.1, 107.5, 104.6, 56.4, 56.3, 54.2, 45.6, 39.0, 34.7, 33.8, 33.5, 32.6, 29.8; HRESIMS m/z 417.2161 $[\text{M} + \text{H}]^+$ (calcd for $\text{C}_{26}\text{H}_{29}\text{N}_2\text{O}_3$, 417.2178).

Compound **13**, amorphous powder, 68% yield; ^1H NMR (400 MHz, CDCl_3) δ 7.89 (s, 1H), 7.87 (s, 1H), 7.48 (dd, $J = 6.8, 2.4$ Hz, 1H), 7.19–7.17 (m, 2H), 7.02 (d, $J = 2.8$ Hz, 1H), 6.87 (s, 1H), 3.96 (s, 3H), 3.91 (s, 3H), 3.84–3.78 (m, 2H), 3.32 (q, $J = 7.6$ Hz, 1H), 2.84–2.72 (m, 4H), 2.68 (s, 3H), 2.00–1.97 (m, 1H), 1.94–1.90 (m, 2H), 1.57–1.37 (m, 4H); ^{13}C NMR (100 MHz, CDCl_3) δ 207.8, 155.9, 155.7, 149.7, 149.4, 148.9, 143.3, 135.1, 129.4, 129.1, 127.7, 123.3, 122.3, 109.6, 107.5, 104.6, 56.4, 56.2, 50.3, 50.2, 45.4, 38.8, 34.5, 33.5, 32.9, 31.8, 25.0; HRESIMS m/z 431.2322 $[\text{M} + \text{H}]^+$ (calcd for $\text{C}_{27}\text{H}_{31}\text{N}_2\text{O}_3$, 431.2335).

Compound **14**, amorphous powder, 89% yield; ^1H NMR (400 MHz, CDCl_3) δ 7.35–7.31 (m, 3H), 7.04 (d, $J = 8.0$ Hz, 2H), 6.95 (s, 1H), 6.90 (t, $J = 7.6$ Hz, 1H), 4.04 (s, 3H), 3.99 (s, 3H), 3.81–3.74 (m, 1H), 3.39–3.32 (m, 1H), 2.85–2.81 (m, 2H), 2.79–2.75 (m, 2H), 2.09–2.00 (m, 1H), 1.97–1.88 (m, 2H), 1.60–1.44 (m, 4H); ^{13}C NMR (100 MHz, CDCl_3) δ 207.8, 155.7, 152.0, 149.6, 148.8, 129.4, 129.2, 119.5, 116.7, 107.5, 104.6, 56.3, 56.2, 50.1, 50.0, 45.4, 38.8, 34.5, 33.5, 33.0, 31.9; HRESIMS m/z 366.2050 $[\text{M} + \text{H}]^+$ (calcd for $\text{C}_{23}\text{H}_{28}\text{NO}_3$, 366.2069).

Compound **15**, amorphous powder, 90% yield; ^1H NMR (400 MHz, CDCl_3) δ 7.18 (s, 1H), 7.06 (d, $J = 8.4$ Hz, 2H), 6.86

(s, 1H), 6.87 (d, $J = 8.4$ Hz, 2H), 3.97 (s, 3H), 3.91 (s, 3H), 3.29 (q, $J = 8.0$ Hz, 1H), 2.78–2.62 (m, 4H), 2.26 (s, 3H), 1.99–1.93 (m, 1H), 1.89–1.79 (m, 2H), 1.50–1.42 (m, 2H), 1.53–1.34 (m, 4H); ^{13}C NMR (100 MHz, CDCl_3) δ 207.9, 155.7, 150.0, 149.7, 148.9, 129.8, 129.5, 129.1, 117.2, 107.6, 104.6, 56.4, 56.3, 50.9, 50.8, 45.6, 38.9, 34.6, 33.6, 33.2, 32.0, 20.5; HRESIMS m/z 380.2210 $[\text{M} + \text{H}]^+$ (calcd for $\text{C}_{24}\text{H}_{30}\text{NO}_3$, 380.2226).

Compound **16**, amorphous powder, 88% yield; ^1H NMR (400 MHz, CDCl_3) δ 7.18 (s, 1H), 7.14 (t, $J = 7.6$ Hz, 1H), 6.87 (s, 1H), 6.76 (d, $J = 8.6$ Hz, 2H), 6.66 (d, $J = 7.6$ Hz, 1H), 3.97 (s, 3H), 3.91 (s, 3H), 3.71–3.66 (m, 2H), 3.31 (q, $J = 8.0$ Hz, 1H), 2.78–2.67 (m, 4H), 2.31 (s, 3H), 1.99–1.94 (m, 1H), 1.89–1.79 (m, 2H), 1.52–1.34 (m, 4H); ^{13}C NMR (100 MHz, CDCl_3) δ 207.8, 155.7, 152.1, 149.6, 148.9, 138.9, 129.5, 129.1, 120.5, 117.7, 113.9, 107.6, 104.7, 56.4, 56.4, 56.3, 50.3, 45.5, 39.0, 34.6, 33.6, 33.2, 32.0, 22.0; HRESIMS m/z 380.2213 $[\text{M} + \text{H}]^+$ (calcd for $\text{C}_{24}\text{H}_{30}\text{NO}_3$, 380.2226).

Compound **17**, amorphous powder, 92% yield; ^1H NMR (400 MHz, CDCl_3) δ 7.29–7.26 (m, 2H), 7.19 (s, 1H), 6.91–6.89 (m, 2H), 6.87 (s, 1H), 3.97 (s, 3H), 3.91 (s, 3H), 3.69–3.63 (m, 2H), 3.31 (q, $J = 8.0$ Hz, 1H), 2.79–2.73 (m, 2H), 2.72–2.64 (m, 2H), 1.99–1.93 (m, 1H), 1.89–1.79 (m, 2H), 1.52–1.41 (m, 4H), 1.29 (s, 9H); ^{13}C NMR (100 MHz, CDCl_3) δ 207.8, 155.7, 149.6, 148.9, 142.2, 129.5, 126.0, 125.9, 116.4, 107.5, 104.6, 56.4, 56.3, 50.4, 50.3, 45.5, 38.9, 34.5, 34.1, 33.5, 33.2, 32.0, 31.6; HRESIMS m/z 422.2681 $[\text{M} + \text{H}]^+$ (calcd for $\text{C}_{27}\text{H}_{36}\text{NO}_3$, 422.2695).

Compound **18**, amorphous powder, 77% yield; ^1H NMR (400 MHz, CDCl_3) δ 7.18 (s, 1H), 6.94 (d, $J = 9.2$ Hz, 2H), 6.87 (s, 1H), 6.84 (d, $J = 9.2$ Hz, 2H), 3.97 (s, 3H), 3.91 (s, 3H), 3.77 (s, 3H), 3.55–3.50 (m, 2H), 3.26 (q, $J = 8.0$ Hz, 1H), 2.78–2.71 (m, 2H), 2.68–2.60 (m, 2H), 2.00–1.93 (m, 1H), 1.90–1.80 (m, 2H), 1.54–1.35 (m, 4H); ^{13}C NMR (100 MHz, CDCl_3) δ 207.9, 155.7, 153.9, 149.7, 148.9, 146.5, 129.5, 119.0, 114.6, 107.6, 104.7, 56.4, 56.3, 55.7, 51.8, 45.5, 38.9, 34.4, 33.5, 33.3, 32.1; HRESIMS m/z 396.2160 $[\text{M} + \text{H}]^+$ (calcd for $\text{C}_{24}\text{H}_{30}\text{NO}_4$, 396.2175).

Compound **19**, amorphous powder, 75% yield; ^1H NMR (400 MHz, CDCl_3) δ 7.18 (s, 1H), 6.98–6.95 (m, 1H), 6.94–6.90 (m, 2H), 6.90–6.86 (m, 2H), 3.97 (s, 3H), 3.91 (s, 3H), 3.59–3.54 (m, 2H), 3.27 (q, $J = 9.2$ Hz, 1H), 2.80–2.72 (m, 2H), 2.70–2.63 (m, 2H), 2.02–1.87 (m, 2H), 1.88–1.74 (m, 2H), 1.60 (s, 1H), 1.50 (m, 2H); ^{13}C NMR (100 MHz, CDCl_3) δ 207.8, 155.8, 149.7, 148.9, 148.8 (d, $J = 2.4$ Hz), 129.5, 118.6 (d, $J = 10$ Hz), 115.7 (d, $J = 20$ Hz), 107.6, 104.7, 56.4, 56.3, 51.3, 45.5, 38.9, 34.4, 33.6, 33.2, 32.1; HRESIMS m/z 384.1961 $[\text{M} + \text{H}]^+$ (calcd for $\text{C}_{23}\text{H}_{27}\text{FNO}_3$, 384.1975).

Compound **20**, amorphous powder, 68% yield; ^1H NMR (400 MHz, CDCl_3) δ 7.19 (d, $J = 5.2$ Hz, 1H), 7.15 (dd, $J = 8.3$, 7.1 Hz, 1H), 6.87 (s, 1H), 6.69 (dd, $J = 6.0$, 2.4 Hz, 1H), 6.61 (dt, $J = 12.8$, 2.4 Hz, 1H), 6.51–6.46 (m, 1H), 3.97 (s, 3H), 3.91 (s, 3H), 3.73–3.68 (m, 2H), 3.29 (q, $J = 8.0$ Hz, 1H), 2.78–2.71 (m, 4H), 1.98–1.91 (m, 1H), 1.89–1.79 (m, 2H), 1.60–1.36 (m, 4H); ^{13}C NMR (100 MHz, CDCl_3) δ 207.8, 164.1 (d, $J = 240$ MHz), 155.8, 153.5 (d, $J = 10$ MHz), 149.7, 148.9, 130.2 (d, $J = 10$ MHz), 129.5, 111.7, 107.6, 105.5 (d, $J = 20$ MHz), 104.7, 103.1 (d, $J = 20$ MHz), 56.4, 56.3, 49.6, 49.6, 45.5, 38.9, 34.5, 33.6, 32.8, 31.7; HRESIMS m/z 384.1967 $[\text{M} + \text{H}]^+$ (calcd for $\text{C}_{23}\text{H}_{27}\text{FNO}_3$, 384.1975).

Compound **21**, amorphous powder, 77% yield; ^1H NMR (400 MHz, CDCl_3) δ 7.47 (d, $J = 8.4$ Hz, 2H), 7.18 (s, 1H), 6.94

(d, $J = 8.4$ Hz, 2H), 6.87 (s, 1H), 3.97 (s, 3H), 3.91 (s, 3H), 3.84–3.79 (m, 2H), 3.30 (q, $J = 8.0$, 1H), 2.86–2.81 (m, 2H), 2.80–2.71 (m, 2H), 1.98–1.91 (m, 1H), 1.90–1.69 (m, 2H), 1.60–1.35 (m, 4H); ^{13}C NMR (100 MHz, CDCl_3) δ 207.7, 155.8, 153.7, 149.8, 148.9, 129.5, 126.6 (q, $J = 4$ Hz), 114.9, 111.5, 107.6, 104.7, 100.6, 56.5, 56.3, 48.9, 48.9, 45.4, 38.9, 34.5, 33.6, 32.6, 31.6; HRESIMS m/z 434.1930 $[\text{M} + \text{H}]^+$ (calcd for $\text{C}_{24}\text{H}_{27}\text{F}_3\text{NO}_3$, 434.1943).

Compound **22**, amorphous powder, 72% yield; ^1H NMR (400 MHz, CDCl_3) δ 7.32 (t, $J = 8.0$ Hz, 1H), 7.18 (s, 1H), 7.12 (t, $J = 2.0$ Hz, 1H), 7.08–7.01 (m, 2H), 6.87 (s, 1H), 3.96 (s, 3H), 3.91 (s, 3H), 3.76–3.70 (m, 2H), 3.27 (q, $J = 7.6$ Hz, 1H), 2.81–2.71 (m, 4H), 1.98–1.93 (m, 1H), 1.91–1.82 (m, 2H), 1.50–1.35 (m, 4H); ^{13}C NMR (100 MHz, CDCl_3) δ 207.7, 155.8, 152.0, 149.7, 148.9, 131.5 (q, $J = 30$ MHz), 129.7, 129.5, 124.6 (q, $J = 280$ MHz) 119.4, 115.5 (q, $J = 10$ MHz), 112.6 (q, $J = 10$ MHz), 107.6, 104.6, 56.4, 56.3, 49.7, 49.6, 45.4, 38.8, 34.4, 33.6, 32.8, 31.7; HRESIMS m/z 434.1935 $[\text{M} + \text{H}]^+$ (calcd for $\text{C}_{24}\text{H}_{27}\text{F}_3\text{NO}_3$, 434.1943).

Compound **23**, amorphous powder, 50% yield; ^1H NMR (400 MHz, CDCl_3) δ 7.24 (d, $J = 3.5$ Hz, 3H), 7.18 (s, 1H), 6.88 (s, 1H), 3.97 (s, 3H), 3.92 (s, 3H), 3.85–3.76 (m, 2H), 3.34–3.21 (m, 1H), 2.86 (m, 2H), 2.81–2.70 (m, 2H), 1.99–1.93 (m, 1H), 1.92–1.85 (m, 2H), 1.49–1.36 (m, 4H); ^{13}C NMR (100 MHz, CDCl_3) δ 207.6, 155.8, 152.1, 149.8, 148.8, 132.4 (q, $J = 30$ MHz), 129.5, 124.9, 121.8, 115.1, 110.6, 107.6, 104.7, 56.5, 56.3, 49.1, 49.0, 45.3, 38.8, 34.3, 33.6, 32.5, 31.5; HRESIMS m/z 502.1801 $[\text{M} + \text{H}]^+$ (calcd for $\text{C}_{25}\text{H}_{26}\text{F}_6\text{NO}_3$, 502.1817).

Compound **24**, amorphous powder, 79% yield; ^1H NMR (400 MHz, CDCl_3) δ 7.60–7.58 (m, 2H), 7.42 (t, $J = 7.6$ Hz, 2H), 7.35–7.30 (m, 2H), 7.19 (s, 1H), 7.16 (t, $J = 2.0$ Hz, 1H), 7.07 (d, $J = 7.6$ Hz, 1H), 6.95 (dd, $J = 8.2$, 2.4 Hz, 1H), 6.87 (s, 1H), 3.96 (s, 3H), 3.91 (s, 3H), 3.80–3.75 (m, 2H), 3.27 (q, $J = 7.6$ Hz, 1H), 2.80–2.73 (m, 4H), 2.08–2.04 (m, 1H), 1.95–1.85 (m, 2H), 1.60–1.42 (m, 4H); ^{13}C NMR (100 MHz, CDCl_3) δ 207.8, 155.7, 152.4, 149.7, 148.9, 142.4, 142.1, 129.6, 129.5, 128.8, 127.4, 127.3, 118.6, 115.8, 115.7, 107.6, 104.6, 56.4, 56.3, 50.3, 50.3, 45.5, 38.9, 34.6, 33.6, 33.1, 31.9; HRESIMS m/z 442.2370 $[\text{M} + \text{H}]^+$ (calcd for $\text{C}_{29}\text{H}_{32}\text{NO}_3$, 442.2382).

Compound **25**, amorphous powder, 69% yield; ^1H NMR (400 MHz, CDCl_3) δ 7.55 (d, $J = 7.2$ Hz, 2H), 7.52 (d, $J = 8.8$ Hz, 2H), 7.40 (t, $J = 8.8$ Hz, 2H), 7.40 (t, $J = 7.6$ Hz, 2H), 7.29–7.27 (m, 1H), 7.19 (s, 1H), 7.02 (d, $J = 8.8$ Hz, 1H), 6.88 (s, 1H), 3.97 (s, 3H), 3.92 (s, 3H), 3.79–3.74 (m, 1H), 3.28 (q, $J = 8.4$ Hz, 1H), 2.81–2.72 (m, 4H), 2.01–1.94 (m, 1H), 1.92–1.82 (m, 2H), 1.52–1.37 (m, 4H); ^{13}C NMR (100 MHz, CDCl_3) δ 207.9, 155.8, 151.2, 149.7, 148.9, 141.2, 132.1, 129.5, 128.9, 127.9, 126.7, 126.5, 116.7, 107.6, 104.7, 56.4, 56.3, 50.0, 45.5, 38.9, 34.6, 33.6, 33.0, 31.9, 29.9; HRESIMS m/z 442.2391 $[\text{M} + \text{H}]^+$ (calcd for $\text{C}_{29}\text{H}_{32}\text{NO}_3$, 442.2382).

Compound **26**, amorphous powder, 80% yield; ^1H NMR (400 MHz, CDCl_3) δ 8.24 (d, $J = 8.0$ Hz, 1H), 8.20 (d, $J = 8.0$ Hz, 1H), 7.53–7.45 (m, 2H), 7.21 (s, 1H), 7.02 (d, $J = 8.0$ Hz, 1H), 6.89 (s, 1H), 6.74 (d, $J = 7.6$ Hz, 1H), 3.97 (s, 6H), 3.92 (s, 3H), 3.34–3.28 (m, 2H), 2.82–2.78 (m, 2H), 2.09–2.04 (m, 1H), 1.95–1.85 (m, 2H), 1.68–1.60 (m, 6H), 1.50–1.42 (m, 1H); ^{13}C NMR (100 MHz, CDCl_3) δ 208.0, 155.7, 151.6, 149.7, 149.0, 144.5, 130.3, 129.6, 129.0, 126.7, 126.2, 125.4, 123.6, 122.5, 114.6, 107.6, 104.7, 103.6, 56.4, 56.3, 55.8, 54.0, 45.8, 33.6, 32.9, 29.9; HRESIMS m/z 446.2319 $[\text{M} + \text{H}]^+$ (calcd for $\text{C}_{28}\text{H}_{32}\text{NO}_4$, 446.2331).

4.2 Biological methods

4.2.1 AChE and BuChE inhibition

All reagents, AChE (from electric eel) and BuChE (from equine serum) were purchased from Sigma-Aldrich. Ellman's method was used to measure the ChE inhibitory effects of synthesized *N*-aryl-debenzyl-donepezils (Ellman et al., 1961). The tested compounds were dissolved in DMSO and diluted with phosphate buffer to final concentrations. The enzyme solution was prepared by dissolving 2.5 mg (0.5 U/mL) AChE in 1 mL pH 8.0 phosphate buffer. In 96-well plates, 140 μ L phosphate buffer (pH 6.7) and 10 μ L AChE were incubated with 10 μ L of various concentrations of test compounds at 25°C for 20 min. Then, 10 μ L DTNB (0.75 mM) and 10 μ L ATCI (1.5 mM) were added for incubation at 37°C for 20 min. The absorbance was monitored at 405 nm using a microplate reader (TECAN SPECTRA, Wetzlar, Germany). Each concentration was assayed in triplicate. BuChE assays were present using a similar method to that described above. Enzyme inhibitory activity (%) = $[1 - (A_{\text{sample}}/A_{\text{control}})] \times 100$.

4.2.2 Cell culture and treatment

The neuroprotective activity was evaluated in human neuroblastoma SH-SY5Y cells which were treated with H₂O₂. Human SH-SY5Y neuroblastoma cells were obtained from ATCC (Manassas, VA, United States) and were cultured at 37°C in a humidified atmosphere of 5% CO₂, in Gibcotm Dulbecco's Modified Eagle Medium (DMEM) supplemented with 10% heat-inactivated fetal bovine serum. The viability of the cells was determined by MTT assay. MTT was purchased from Sigma-Aldrich (St. Louis, MO, United States). SH-SY5Y cells were seeded in 96-well plates at a density of 1×10^5 cells/well for 12 h. Cells were pretreated with 50 μ M of each test compound. After 24 h of incubation, hydrogen peroxide solution (H₂O₂, 700 μ M) was added and incubated for 4 h. Then, MTT (5 mg/mL) was added to each well. After a 4 h treatment, the supernatant was removed, and DMSO (150 μ L/well) was added to dissolve the insoluble formazan crystals. Then, the plate was vibrated, and the absorbance was measured at 490 nm using a microplate reader.

4.2.3 Molecular docking analysis

The ligand-protein docking was guided by Discovery Studio 2020 Client and PyRx software to predict the binding poses of the ligand in the active site of AChE. The 3D models of AChE (PDB ID: 1acj) and BuChE (PDB ID: 6ASM) were obtained from Protein Data Bank (<http://www.rcsb.org/>). The 3D models of the protein of AchE and BuChE were further optimized by Discovery Studio 2020 Client to minimize energy. The AutoDock Vina was employed for docking calculations using the default parameters. The blood-brain barrier (BBB) penetration was predicted by the Discovery Studio 2020 Client.

Data availability statement

The raw data supporting the conclusion of this article will be made available by the authors, without undue reservation.

Author contributions

J-JX: Formal Analysis, Funding acquisition, Writing–review and editing. JL: Methodology, Software, Writing–review and editing. HX: Formal Analysis, Writing–review and editing. J-BX: Methodology, Writing–original draft, Writing–review and editing. L-XW: Conceptualization, Funding acquisition, Supervision, Writing–original draft, Writing–review and editing.

Funding

The author(s) declare financial support was received for the research, authorship, and/or publication of this article. This research was financially supported by grants from the National Natural Science Foundation of China (82204244), the Natural Science Foundation of Sichuan Province (23NSFSC2370), and the Young Pharmacist Foundation of Sichuan Hospital Association (22031).

Conflict of interest

The authors declare that the research was conducted in the absence of any commercial or financial relationships that could be construed as a potential conflict of interest.

Publisher's note

All claims expressed in this article are solely those of the authors and do not necessarily represent those of their affiliated organizations, or those of the publisher, the editors and the reviewers. Any product that may be evaluated in this article, or claim that may be made by its manufacturer, is not guaranteed or endorsed by the publisher.

Supplementary material

The Supplementary Material for this article can be found online at: <https://www.frontiersin.org/articles/10.3389/fchem.2023.1282978/full#supplementary-material>

References

- Akhood, B. A., Choudhary, S., Tiwari, H., Kumar, A., Barik, M. R., Rathor, L., et al. (2020). Discovery of a new donepezil-like acetylcholinesterase inhibitor for targeting Alzheimer's disease: computational studies with biological validation. *J. Chem. Inf. Model.* 60, 4717–4729. doi:10.1021/acs.jcim.0c00496
- Anand, P., and Singh, B. (2013). A review on cholinesterase inhibitors for Alzheimer's disease. *Arch. Pharm. Res.* 36, 375–399. doi:10.1007/s12272-013-0036-3
- Cheung, J., Rudolph, M. J., Burshteyn, F., Cassidy, M. S., Gary, E. N., Love, J., et al. (2012). Structures of human acetylcholinesterase in complex with pharmacologically important ligands. *J. Med. Chem.* 55, 10282–10286. doi:10.1021/jm300871x
- Coleman, P., Federoff, H., and Kurlan, R. (2004). A focus on the synapse for neuroprotection in Alzheimer disease and other dementias. *Neurology* 63, 1155–1162. doi:10.1212/01.wnl.0000140626.48118.0a

- Dorel, R., Grugel, C. P., and Haydl, A. M. (2019). The Buchwald-Hartwig amination after 25 years. *Angew. Chem. Int. Ed.* 58, 17118–17129. doi:10.1002/anie.201904795
- Du, C. X., Wang, L., Guan, Q. W., Yang, H. Y., Chen, T. K., Liu, Y. J., et al. (2022). *N*-benzyl benzamide derivatives as selective sub-nanomolar butyrylcholinesterase inhibitors for possible treatment in advanced Alzheimer's disease. *J. Med. Chem.* 65, 11365–11387. doi:10.1021/acs.jmedchem.2c00944
- Du, X. G., Wang, X. Y., and Geng, M. Y. (2018). Alzheimer's disease hypothesis and related therapies. *Transl. Neurodegener.* 7, 2. doi:10.1186/s40035-018-0107-y
- Ellman, G. L., Courtney, K. D., Andres, V., Jr., and Featherstone, R. M. (1961). A new and rapid colorimetric determination of acetylcholinesterase activity. *Biochem. Pharmacol.* 7, 88–95. doi:10.1016/0006-2952(61)90145-9
- Heravi, M. M., Kheilkordi, Z., Zadsirjan, V., Heydari, M., and Malmir, M. (2018). Buchwald-Hartwig reaction: an overview. *J. Organomet. Chem.* 861, 17–104. doi:10.1016/j.jorganchem.2018.02.023
- Lee, S. Y., Chiu, Y. J., Yang, S. M., Chen, C. M., Huang, C. C., Lee-Chen, G. J., et al. (2018). Novel synthetic chalcone-coumarin hybrid for A beta aggregation reduction, antioxidant, and neuroprotection. *CNS Neurosci. Ther.* 24, 1286–1298. doi:10.1111/cns.13058
- Li, Q., Xing, S. S., Chen, Y., Liao, Q. H., Xiong, B. C., He, S. Y., et al. (2020). Discovery and biological evaluation of a novel highly potent selective butyrylcholinesterase inhibitor. *J. Med. Chem.* 63, 10030–10044. doi:10.1021/acs.jmedchem.0c01129
- Liu, J., Liu, L., Zheng, L., Feng, K. W., Wang, H. T., Xu, J. P., et al. (2022). Discovery of novel 2,3-dihydro-1H-inden-1-ones as dual PDE4/AChE inhibitors with more potency against neuroinflammation for the treatment of Alzheimer's disease. *J. Med. Chem.* 238, 114503. doi:10.1016/j.jmech.2022.114503
- Miao, S. X., Wan, L. X., He, Z. X., Zhou, X. L., Li, X. H., and Gao, F. (2021). Pd-catalyzed direct diversification of natural anti-Alzheimer's disease drug: synthesis and biological evaluation of *N*-aryl Huperzine A analogues. *J. Nat. Prod.* 84, 2374–2379. doi:10.1021/acs.jnatprod.1c00600
- Mozaffaria, S., Teimuri-Mofrad, R., and Rashidi, M. R. (2020). Design, synthesis and biological evaluation of 2,3-dihydro-5,6-dimethoxy-1H-inden-1-one and piperazinium salt hybrid derivatives as hAChE and hBuChE enzyme inhibitors. *Eur. J. Med. Chem.* 191, 112140. doi:10.1016/j.ejmech.2020.112140
- Niikura, T., Hashimoto, Y., Tajima, H., and Nishimoto, I. (2002). Death and survival of neuronal cells exposed to Alzheimer's insults. *J. Neurosci. Res.* 70, 380–391. doi:10.1002/jnr.10354
- Pardo-Moreno, T., Gonzalez-Acedo, A., Rivas-Dominguez, A., Garcia-Morales, V., Garcia-Cozar, F. J., Ramos-Rodriguez, J. J., et al. (2022). Therapeutic approach to Alzheimer's disease: current treatments and new perspectives. *Pharmaceutics* 14, 1117. doi:10.3390/pharmaceutics14061117
- Peauger, L., Azzouz, R., Gembus, V., Tintas, M. L., Santos, J. S. D., Bohn, P., et al. (2017). Donepezil-based central acetylcholinesterase inhibitors by means of a "bio-oxidizable" prodrug strategy: design, synthesis, and *in vitro* biological evaluation. *J. Med. Chem.* 60, 5909–5926. doi:10.1021/acs.jmedchem.7b00702
- Perry, G., Cash, A. D., and Smith, M. A. (2002). Alzheimer disease and oxidative stress. *J. Biomed. Sci.* 15, 120–123. doi:10.1155/S1110724302203010
- Qian, H. J., Yu, C. Y., Zhu, H. J., Ding, Q. C., Cai, Y. T., Jing, J., et al. (2023). Safety, tolerability, and pharmacokinetics of fluoropezil (DC20), a novel acetylcholinesterase inhibitor: A phase I study in healthy young and elderly Chinese subjects. *CTS-Clin. Transl. Sci.* 16, 810–822. doi:10.1111/cts.13490
- Ross, C. A., and Poirier, M. A. (2004). Protein aggregation and neurodegenerative disease. *Nat. Med.* 10, 10–17. doi:10.1038/nm1066
- Seltzer, B. (2007). Donepezil: an update. *Expert Opin. Pharmacother.* 8, 1011–1023. doi:10.1517/14656566.8.7.1011
- Summers, W. K., Koehler, A. L., Marsh, G. M., Tachiki, K., and Kling, A. (1989). Long-term hepatotoxicity of tacrine. *Lancet* 1, 729. doi:10.1016/s0140-6736(89)92246-0
- Wan, L. X., Miao, S. X., He, Z. X., Li, X. H., Zhou, X. L., and Gao, F. (2021a). Pd-catalyzed direct modification of an anti-Alzheimer's disease drug: synthesis and biological evaluation of α -aryl donepezil analogues. *ACS Omega* 6, 23347–23354. doi:10.1021/acsomega.1c03103
- Wan, L. X., Zhang, J. F., Zhen, Y. Q., Zhang, L., Li, X. H., Gao, F., et al. (2021b). Isolation, structure elucidation, semi-synthesis, and structural modification of C₁₉-diterpenoid alkaloids from *Aconitum apetalum* and their neuroprotective activities. *J. Nat. Prod.* 84, 1067–1077. doi:10.1021/acs.jnatprod.0c01111
- Wan, L. X., Zhen, Y. Q., He, Z. X., Zhang, Y., Zhang, L., Li, X. H., et al. (2021c). Late-stage modification of medicine: Pd-catalyzed direct synthesis and biological evaluation of *N*-aryltacrine derivatives modification of medicine: Pd-catalyzed direct synthesis and biological evaluation of *N*-aryltacrine derivatives. *ACS Omega* 6, 9960–9972. doi:10.1021/acsomega.1c01404
- Xu, J. B., Miao, S. X., Gao, F., and Wan, L. X. (2023). Palladium-catalyzed synthesis and acetylcholinesterase inhibitory activity evaluation of 1-arylhuperzine A derivatives acetylcholinesterase inhibitory activity evaluation of 1-arylhuperzine A derivatives. *J. Asian Nat.* 25, 1097–1109. doi:10.1080/10286020.2023.2196619
- Zhang, Y., Xu, J. B., Xiao, Y., Ji, W. S., Shan, L. H., Wan, L. X., et al. (2023). Palladium-Catalyzed synthesis, acetylcholinesterase inhibition and neuroprotective activities of *N*-aryl galantamine analogues. *J. Nat. Prod.* 86, 939–946. doi:10.1021/acs.jnatprod.2c01150
- Zhou, Y., Fu, Y., Yin, W. C., Li, J., Wang, W., Bai, F., et al. (2021). Kinetics-driven drug design strategy for next-generation acetylcholinesterase inhibitors to clinical candidate. *J. Med. Chem.* 64, 1844–1855. doi:10.1021/acs.jmedchem.0c01863